AJNR

Assessment of Dural Arteriovenous Fistulas of the Cavernous Sinuses on 3D Dynamic MR Angiography

H. Akiba, M. Tamakawa, H. Hyodoh, K. Hyodoh, N. Yama, T. Nonaka, Y. Minamida, M. Hashimoto and M. Hareyama

AJNR Am J Neuroradiol 2008, 29 (9) 1652-1657
doi: https://doi.org/10.3174/ajnr.A1187
http://www.ajnr.org/content/29/9/1652

ORIGINAL RESEARCH

Assessment of Dural Arteriovenous Fistulas of the Cavernous Sinuses on 3D Dynamic MR Angiography

H. Akiba
M. Tamakawa
H. Hyodoh
K. Hyodoh
N. Yama
T. Nonaka
Y. Minamida
M. Hashimoto
M. Hareyama

BACKGROUND AND PURPOSE: Flow voids within the cavernous sinuses and/or certain venous drainage on spin-echo MR imaging and time-of-flight (TOF) flow enhancement on MR angiography (MRA) have indicated high-velocity shunt flow and have been used for screening patients with dural arteriovenous fistulas (DAVFs) of the cavernous sinuses. In this investigation, the capabilities of 3D dynamic MRA as a flow-independent approach and those of conventional MR imaging techniques were compared with selective angiography for the diagnosis of DAVFs of the cavernous sinuses.

MATERIALS AND METHODS: This retrospective study involved 18 patients with angiographically proved DAVFs of the cavernous sinuses and 12 control subjects. Sixteen partially overlapping sequential MR images were acquired on contrast-enhanced 3D dynamic MRA between the petrosal bone and the orbital roof. Two experienced observers blinded to the clinical data and results of angiography independently graded 3D dynamic MRA, fast spin-echo T2-weighted imaging (FSE T2WI), and TOF MRA.

RESULTS: The average area under the receiver operating characteristic curve values and interobserver κ scores for the diagnosis of DAVFs on 3D dynamic MRA, FSE T2WI, and TOF MRA were 0.99, 0.89, and 0.95; and 0.92, 0.71, and 0.73, respectively. Those for the diagnosis of anterior, posterior, and retrograde cortical venous drainage on 3D dynamic MRA were 0.72, 0.95, and 0.81; and 0.56, 0.50, and 0.49, respectively.

CONCLUSION: In this small series, screening 3D dynamic MRA directly demonstrates DAVFs of the cavernous sinuses and has improved diagnostic capability.

In patients with the classic triad of pulsating exophthalmos, orbital bruit, and conjunctival chemosis, the clinical diagnosis of arteriovenous fistulas (AVFs) of the cavernous sinuses is not difficult, and cerebral angiography is performed for definitive diagnosis. However, dural AVFs (DAVFs) without anterior drainage may not cause typical congestive orbito-ocular features, and thrombosis of the draining veins may lead to spontaneous resolution of the disorder.[1-6] Therefore, it is desirable to perform less invasive diagnostic examinations before conventional angiography. So far, flow voids within the cavernous sinuses and/or inferior petrosal sinuses on spin-echo MR images followed by time of flight (TOF) flow enhancement on source images of MR angiography (MRA) have been indicative of AVF.[7-10] Although these are safe and practical methods, dependence on flow velocity sometimes makes it impossible to distinguish fast normal flow from abnormal shunt flow or slow abnormal shunt flow from normal flow.[9-13]

The recent advancement of MR imaging technology has allowed first-pass contrast-enhanced dynamic MRA and 2D MR digital subtraction angiography to be applied to cerebral arteriovenous malformations (AVMs) or DAVFs.[14-18] In addition, although the conventional use of 3D dynamic MRA for their diagnosis has been difficult due to the limitation of low temporal resolution, its application has been described in recently published articles.[19,20] However, until now, there has not been a comparative study of dynamic MRA and conventional MR imaging for the diagnosis of DAVFs of the cavernous sinuses.

According to a study of dynamic CT of the cavernous sinuses[21] and physiologic studies on the cerebral circulation time,[22,23] it was hypothesized that imaging temporal resolution under several seconds would demonstrate DAVFs of the cavernous sinuses on dynamic MRA. Therefore, we used the 3D data-acquisition technique, a standard pulse sequence, and postulated that early enhancement of the cavernous sinuses was a main direct feature of the shunts. This methodology will improve the diagnostic capability for screening of DAVFs of the cavernous sinuses.

Materials and Methods

Patients and Control Subjects

From September 1999 to May 2006, 70 consecutive MR imaging studies focused on the diagnosis of AVFs of the cavernous sinuses were performed in 49 patients at our institution. The selection criteria in this retrospective case-control study were as follows: a clinical suggestion of or a previous history of AVFs of the cavernous sinuses. Studies that were performed to exclude AVFs of the cavernous sinuses were also selected. Forty MR imaging studies in 19 patients were excluded for the following reasons: 7 in 6 patients with direct carotid cavernous sinus fistulas, 2 in 2 patients with AVFs unrelated to the cavernous sinuses, 8 in 8 patients who remained undiagnosed, and 9 in 3 patients who underwent MR imaging only after treatment for DAVFs of the

Received January 22, 2008; accepted after revision May 7.

From the Departments of Radiology (H.A., M.T., H.H., K.H., N.Y., M. Hareyama), Neurosurgery (T.N., Y.M.), and Ophthalmology (M. Hashimoto), Sapporo Medical University, School of Medicine, Sapporo, Japan.

Paper previously presented as a poster at: 89th Scientific Assembly and Annual Meeting of the Radiological Society of North America, November 30–December 5, 2003; Chicago, Ill; and as a scientific exhibit (digital poster) at: Annual Meeting of the European Society of Radiology, May 7–11, 2008; Vienna, Austria.

Please address correspondence to Hidenari Akiba. MD, PhD, Department of Radiology, Sapporo Medical University, School of Medicine, W-16, S-1, Chuo-ku, Sapporo, 060-0061, Japan; e-mail akibah@sapmed.ac.jp

DOI 10.3174/ajnr.A1187

cavernous sinuses. Then, 14 re-examinations after treatment for DAVFs of the cavernous sinuses were also excluded. Thus, 30 MR imaging studies in 30 patients were included in this investigation.

DAVFs of the cavernous sinuses were confirmed by angiography in 18 patients (3 men and 15 women; age range, 41–81 years; mean age, 66.1 years) who underwent MR imaging before treatment, and 11 were re-examined for follow-up after treatment. Selective angiographies in these 18 patients were interpreted by 2 experienced radiologists on concurrent observation as follows: bilateral DAVFs were diagnosed in 5 and unilateral DAVFs in 13; anterior, posterior, inferior, and contralateral drainage was demonstrated in 13, 10, 5, and 6 patients, respectively; and venous sinus drainage with cortical reflux was observed in 9 patients. According to the classified categories of Borden et al,[24] type I and II DAVFs were seen in 9 patients each and there were no patients with type III DAVFs. The time intervals between 3D dynamic MRA and angiography ranged from 2 days to 3 weeks (9.7 days on average) in 17 patients. One patient who underwent angiography twice, 110 days before and 98 days after 3D dynamic MRA, was included in this study because there was no change in clinical manifestations or the results of the 2 studies during this time. Thus, the patient group comprised these 18 patients. Typical orbital congestive features were observed in 12 patients, and the other 6 patients had other nonspecific manifestations such as ophthalmoplegia, headache, and decline of visual acuity.

The other 12 patients (7 men and 5 women; age range, 22–89 years; mean age, 55.8 years) were clinically diagnosed as follows: 2 each had traumatic optic neuropathy and glaucoma; and 1 each had Tolosa-Hunt syndrome, ischemic optic neuropathy, cavernous sinus syndrome, central retinal vein occlusion, optic neuritis, Fisher syndrome, Grave ophthalmopathy, and trigeminal neuralgia. Orbital congestion was noted in 5. The observation periods in these patients ranged from 9 months to 4 years and 7 months (1.7 years on average), and their conditions were considered not to be related to DAVFs of the cavernous sinuses. Then, DAVFs were definitively excluded in 2 patients who underwent angiography at other institutions. Therefore, the control group consisted of these 12 patients.

Thus, among all 30 subjects (patients/controls, 18/12), 24 subjects (14/10) underwent 3D dynamic MRA, 30 subjects (18/12) underwent fast spin-echo T2-weighted imaging (FSE T2WI), and 22 subjects (13/9) underwent TOF MRA.

Imaging Technique

All images were acquired with two 1.5T MR imaging systems. To acquire 16 partially overlapping images on 3D dynamic MRA, a transverse 3D fast spoiled gradient-recalled echo (SPGR) sequence was obtained with the following parameters: TR/TE/flip angle/NEX, 5.5–6.4/1.8–1.9 ms/30°/0.5 (by using a head coil before December 2002) or 4.11/1.33 ms/30°/0.5 (by using an 8-channel head phased-array coil and array spatial sensitivity encoding techniques after January 2003); slab thickness/section thickness/zero-fill interpolation process, 8 cm/1 cm/4; and FOV/matrix size, 20 cm/256 × 128. Considering normal cerebral circulation time, we used the imaging time intervals that ranged from 4 to 5 seconds during the first period and were 2.3 seconds during the second period.[21-23] The total imaging time was 36–60 seconds. Because the 2-section-thicknesses on both ends of a slab were automatically discarded on 3D fast SPGR pulse sequences, a 4-cm scanning range was actually obtained. The cavernous sinuses and the branching parts of the draining veins were included within this 4-cm axial scanning range between the petrosal bone and the orbital roof (1-cm thickness, 2.5-mm interval, 7.5-mm overlap, and 16 sections).

Gadolinium contrast agent 0.1 mmol/kg and 20-mL normal saline were mechanically injected with the 2-cylinder MR imaging injector at 3 mL/s through a 20-gauge needle in an antecubital vein, and the imaging protocol was simultaneously started at the beginning of the injection. When first-pass enhancement of the cerebral arteries was shown without venous enhancement in multiphase/section images, the phases were identified as the arterial-dominant phases, whereas the previous non-contrast-enhanced phase was labeled as the origin and the subsequent phases were labeled as the arteriovenous phases due to enhancement of both arteries and veins. The images in the non-contrast-enhanced phase were used as mask images and subtracted from those in the arterial-dominant phases and subsequent arteriovenous phases. The images in the arterial-dominant phase were observed for this study to come as close as possible to an objective evaluation. When 2 arterial-dominant phases were obtained during the second period, the latter arterial-dominant phase was selected because of distinct visualization of venous drainage.

FSE T2WI was performed with the following parameters: TR/TE/flip angle/section thickness/gap/FOV/matrix size, 4500/100 ms/90°/4 mm/1.5 mm/18–21-cm/512 × 512. Then, the 3D SPGR sequence was used on TOF MRA, and the technical scanning parameters were as follows: TR/TE/flip angle/NEX, 30–40/3.7–5.6 ms/25°–30°; and section thickness/FOV/matrix size, 1 mm/18–21-cm/256 × 128 with fat saturation for MRA or 1.2–3 mm/16–21-cm/256–512 × 128–224 without fat saturation for target T1-weighted images. The latter was obtained before and after administration of contrast material in cases of clinical requirement for differentiation from neoplasm or inflammation. Thus, the source images of MRA in 9 and the target T1-weighted images in 13 were used as TOF MRA.

Imaging Analysis

The imaging data were archived to a workstation after proper adjustment of the window/level for review. Two radiologists independently observed the images of the 3 techniques for each subject without any knowledge of the results of angiography and clinical information. After the order of the subjects for each MR imaging technique was randomized, the images were presented for interpretation. First, the observers reviewed the sequential images of each subject and assessed the presence or absence of DAVFs of the cavernous sinus. The diagnostic criteria for DAVFs of the cavernous sinuses were the following: early enhancement of the cavernous sinuses in the arterial-dominant phase on 3D dynamic MRA, flow voids on FSE T2WI, and high signal intensities on TOF MRA. Diagnosis on FSE T2WI was made if there were enough large flow voids within the cavernous sinuses because small flow voids without shunts were frequently demonstrated on routine examination. Thus, the confidence levels of the readers as to the presence or absence of DAVFs of the cavernous sinuses were recorded by using a continuously distributed scale ranging from 0% (definitely absent) to 100% (definitely present).[25]

In addition, the presence or absence of anterior, posterior, and retrograde cortical venous drainage was evaluated on 3D dynamic MRA. Anterior venous drainage was diagnosed if the superior or inferior ophthalmic veins were enhanced early in the arterial-dominant phase. Posterior venous drainage was assessed if the inferior or superior petrosal sinuses or basilar plexuses were seen. The diagnostic criterion of cortical reflux was early filling of contrast material within the sphenoparietal sinuses or superficial middle cerebral veins. Evaluation of inferior venous drainage was not performed in this study

because the imaging range might not include this area. It was difficult to discriminate DAVFs of the unilateral cavernous sinus draining into the contralateral cavernous sinus from DAVFs of the bilateral cavernous sinuses due to the limitation of the temporal resolution on 3D dynamic MRA, so the evaluation for intercavernous venous drainage was also excluded. Both readers were asked to pay careful attention to differentiation of the draining veins from the adjacent arteries, and they described their degree of confidence for the presence or absence of venous drainage by using the continuously distributed scale.

Statistical Analysis

The accuracies of the interpretation of 3 MR imaging techniques compared with the results of selective angiography and clinical diagnosis were assessed with receiver operating characteristic (ROC) analysis by using the continuously distributed scale.[25] The area under the ROC curve (A_z) is a good summary measure of test accuracy because it does not depend on the prevalence of disease or the cut-points used to form the curve.[26] This analysis was performed by using ROC programs (ROCKIT and LABMRMC, Charles E. Metz; University of Chicago, Chicago, Ill). The sensitivity and specificity were calculated for each observer separately by using the dichotomized data from the ROC analysis: the cut-point was located at 50%, so the scores between 0% and 49% were negative for the presence of DAVFs or their venous drainage and the scores between 50% and 100% were positive. The proportions were calculated with 95% confidence intervals (CIs) based on the F distribution for this small series. The interobserver agreements between the 2 reviewers for the detection of DAVFs of the cavernous sinuses on each MR imaging technique and venous drainage on 3D dynamic MRA were assessed by unweighted κ statistics based on the dichotomization of the data.[27] The level of agreement was defined as follows: κ values of 0–0.19 represented poor agreement; 0.2–0.39, fair; 0.4–0.59, moderate; 0.6–0.79, good; and 0.8–1.00, excellent agreement.

Results

The average A_z values from the 2 readers were 0.99 (95% CI, 0.91–1.00), 0.89 (95% CI, 0.71–0.97), and 0.95 (95% CI, 0.74–1.00) for the diagnosis of DAVFs on 3D dynamic MRA, FSE T2WI, and TOF MRA, respectively; and there was a statistically significant difference in the diagnosis between 3D dynamic MRA and FSE T2WI ($P < .05$). The interobserver κ scores were 0.92 (95% CI, 0.75–1.00), 0.71 (95% CI, 0.45–0.97), and 0.73 (95% CI, 0.44–1.00), respectively. The average sensitivities for both observers were 0.96 (27/28; 95% CI, 0.82–1.00), 0.86 (31/36; 95% CI, 0.71–0.94), and 0.85 (22/26; 95% CI, 0.65–0.96), respectively; and the average specificities were 1.00 (20/20; 95% CI, 0.86–1.00), 0.71 (17/24; 95% CI, 0.49–0.85), and 0.94 (17/18; 95% CI, 0.74–1.00), respectively.

The average A_z values from both readers and interobserver κ scores for the diagnosis of anterior, posterior, and cortical venous drainage on 3D dynamic MRA were 0.72 (95% CI, 0.41–0.92), 0.95 (95% CI, 0.77–1.00), and 0.81 (95% CI, 0.57–0.94); and 0.56 (95% CI, 0.17–0.95), 0.50 (95% CI, 0.15–0.85), and 0.49 (95% CI, 0.14–0.84), respectively. The average sensitivities for both observers were 0.40 (8/20; 95% CI, 0.19–0.64), 1.00 (14/14; 95% CI, 0.81–1.00), and 0.86(12/14; 95% CI, 0.57–0.98), respectively; and the average specificities were 0.86 (24/28; 95% CI, 0.67–0.96), 0.71 (24/34; 95% CI, 0.53–0.85), and 0.53 (18/34; 95% CI, 0.35–0.70), respectively.

Discussion

Non-contrast-enhanced examinations, such as spin-echo MR imaging and subsequent TOF MRA, have been recommended for screening for AVFs of the cavernous sinuses.[7-10] Although highly specific criteria with a low false-negative rate were documented with TOF MRA initially,[10] other studies have found a low false-positive rate[11,12] and an 11% frequency of "pseudoshunt" signals within the cavernous sinuses or inferior petrosal sinuses.[13] These techniques were thought to have low potential for false diagnosis due to dependence on shunt flow velocity. Meanwhile, there is a relationship between nonspecific signs such as isolated ocular motor palsies and venous drainage other than anterior drainage in patients with DAVFs of the cavernous sinuses.[4,5] This presentation occurs in 33% of patients.[6] Therefore, a highly sensitive screening mechanism for the diagnosis of DAVFs of the cavernous sinuses is necessary for patients with these clinical features.

The results of this investigation indicate that DAVFs of the cavernous sinuses are demonstrated directly and flow-independently as early venous filling of contrast material on 3D dynamic MRA (Figs 1 and 2). Both sensitivity and specificity were high, leading to precise diagnosis; and excellent interobserver agreements were revealed. Meanwhile, high diagnostic capability was also documented with TOF MRA, and interobserver agreement was good. As previously reported, the specificity was high and the sensitivity was not so high.[10] That is, attention should be paid to the small number of false-negative results for screening. In addition, until now, there has been no investigation of FSE T2WI after an evaluation of spin-echo T2WI.[10] As a result of this study, there was a certain degree of false diagnoses with screening with FSE T2WI. However, it is an advantage to be able to observe the indirect manifestations of shunting such as orbital congestive features or a rare complication of brain congestion due to cortical venous reflux.[28]

Although the observation of the source sectional images facilitated the identification of the cerebral vessels and might yield information about main venous drainage (Fig 2), the diagnostic capabilities of venous drainage, especially anterior drainage, were not sufficient on 3D dynamic MRA and the interobserver agreements were moderate. The precise reasons for these results are unknown; however, restricted assessment of only arterial-dominant phase images may make it difficult to evaluate slow venous filling.

In this study, 3D dynamic MRA contributed to the diagnosis of DAVFs in 6 patients without typical orbital congestive features and the exclusion of this diagnosis in 5 patients with other diseases presenting with similar signs and symptoms. Thus, 3D dynamic MRA plays a role in screening patients with equivocal clinical features. As a result, we believe that this direct procedure is useful for the diagnosis of latent DAVFs with small shunt flow that are occasionally difficult to visualize on conventional MR imaging. Figure 3 illustrates a diagnostic flow chart of DAVFs of the cavernous sinuses. In patients with the classic triad of symptoms, selective angiography is performed for definitive diagnosis or treatment. Meanwhile, in patients with nonspecific clinical manifestations, including orbital congestion, performing conventional MR imaging first is recommended, followed by 3D dynamic MRA, because we can confirm or exclude DAVFs of the cavernous sinuses but also may obtain information about main venous drainage.

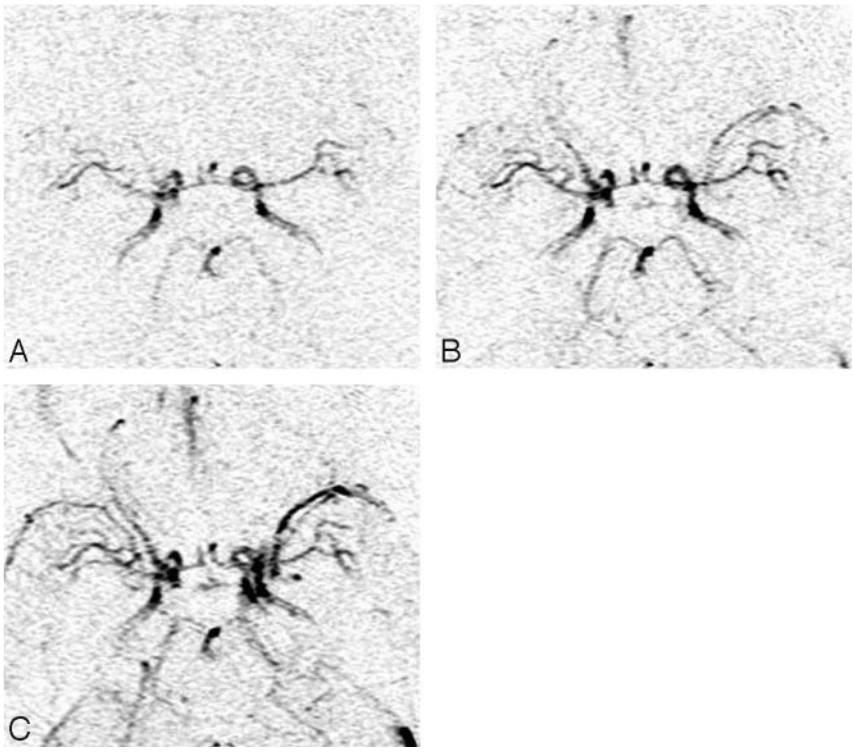

Fig 1. A 52-year-old woman presenting with proptosis and chemosis in the right orbit and 2 months of diplopia resulting from anterior draining DAVFs of the right cavernous sinus. Subtracted maximum-intensity-projection images on 3D dynamic MRA. *A* and *B*, Early venous enhancement is demonstrated within the right cavernous sinus and superior ophthalmic vein in the arterial-dominant phase (*A*) and is more clearly identified in the next phase (*B*). *C*, The venous structures are visualized by normal venous return in the arteriovenous phase.

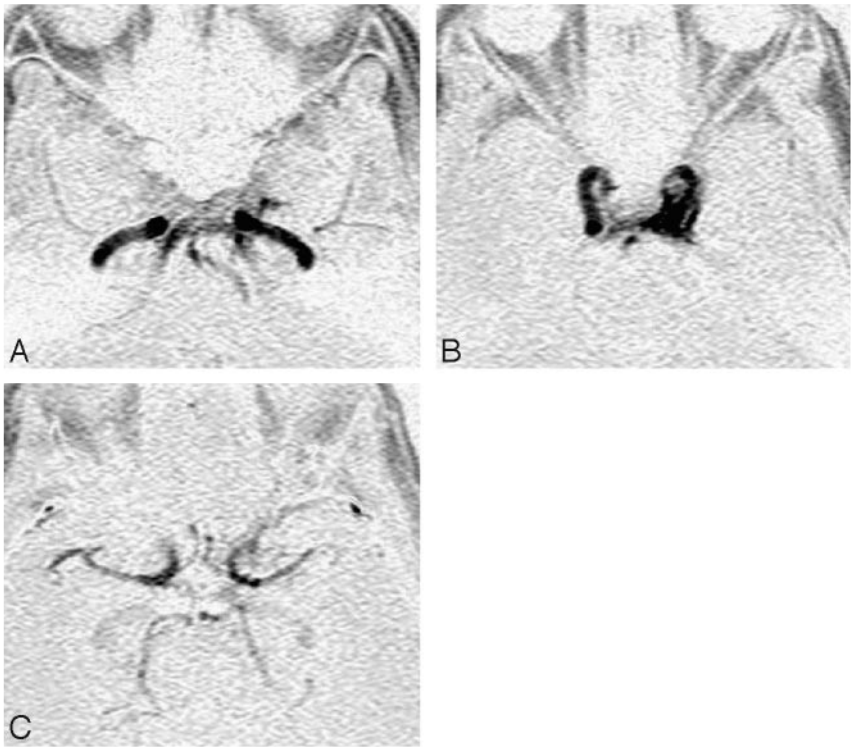

Fig 2. A 65-year-old woman with left frontal pain and diplopia for 1 month without congestive orbito-ocular features resulting from DAVFs of the left cavernous sinus. Reversed source sectional images in the arterial-dominant phase on 3D dynamic MRA. *A* and *B*, Early venous enhancement is demonstrated within the bilateral inferior petrosal sinuses, basilar plexus, left pterygoid plexus (*A*), and left cavernous sinus (*B*). *C*, In addition, retrograde cortical reflux to the left sphenoparietal sinus is a clinically important feature.

Recently, 2D MR digital subtraction angiography in patients with cerebral AVMs or AVFs was found to provide temporal resolution in less than a second and clarified the hemodynamics of the disease in a manner similar to that of conventional angiography.[14-18] Reduction of imaging time facilitates resolution of the cerebral vessels; however, it is funda-

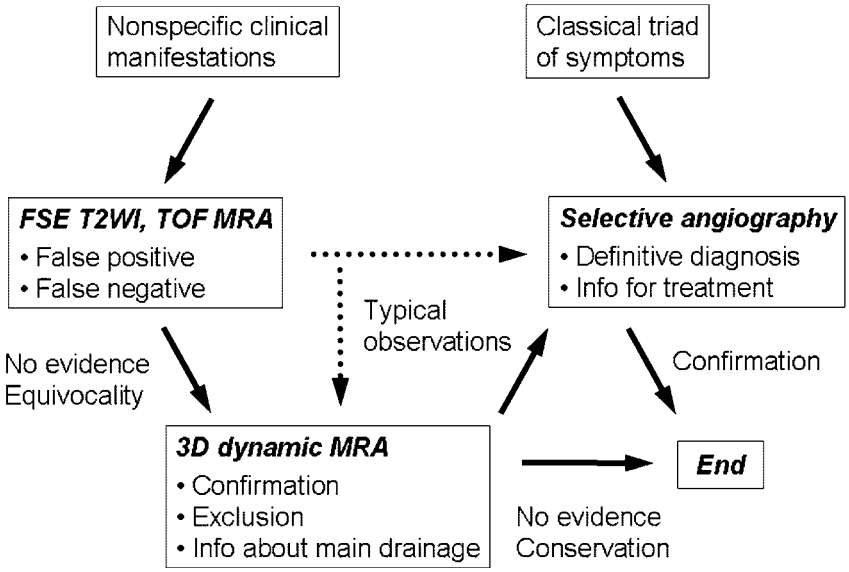

Fig 3. A diagnostic flow chart of DAVFs of the cavernous sinuses.

mentally impossible to display the overlapping vessels separately on a 2D data acquisition. The cerebral vessels within the definite territories are visualized on selective angiography, whereas all intracranial vessels are demonstrated simultaneously through the peripheral intravenous administration of contrast material. In the case of AVMs or AVFs, it is much more difficult to discriminate the crossing vessels because the enhanced arteries and early enhanced draining veins through fistulas overlap in the same phases.

Identification of the draining veins is important for treatment of DAVFs, and reflux to the cortical veins may result in venous infarction or cerebral hemorrhage due to venous hypertension.[2,24,28] With priority given to this point, we used 3D dynamic MRA to obtain spatial information, included the cavernous sinuses and the branching parts of the draining veins within the imaging area, and attempted to improve the spatial resolution as much as possible while minimizing temporal resolution. It was disclosed in a previous article of dynamic CT of the cavernous sinuses that optimal enhancement of the cavernous sinuses occurred 5 seconds after optimal enhancement of the internal carotid arteries, and 10 seconds later the cavernous sinuses appeared homogeneous.[20] In addition, recent investigations indicated that the normal cerebral circulation time was 5–8 seconds.[22,23] According to these studies, the imaging time intervals should be less than several seconds to display early enhancement of the cavernous sinuses with DAVFs. In previous articles on 3D dynamic MRA, the temporal resolution was not enough for this study due to technical limitations. In a recent investigation for the diagnosis of intracranial AVMs,[19] volume data acquisition at a several-second interval was realized; however, the technique is not widely prevalent.

In our study, one of the standard pulse sequences of the MR unit was used, which seemed to be incidentally similar to another recent study for cerebral AVMs.[20] Because the imaging time intervals ranged from 2.3 to 5 seconds on 3D dynamic MRA, it was possible to differentiate the normal branches of the arteries from those of the veins. Then, the appearance of early venous filling of contrast material in the arterial-dominant phases permitted the diagnosis of DAVFs of the cavernous sinuses, and the confirmation of main venous drainage might result from the evaluation of the source sectional images (Fig 2).

There were some limitations in this study: The feeding arteries and entry points could not be demonstrated on 3D dynamic MRA, and it was impossible to differentiate DAVFs of the cavernous sinuses from direct carotid cavernous sinus fistulas or AVFs draining indirectly into the cavernous sinuses. Furthermore, visualization of venous drainage was limited by administration of contrast material through a peripheral vein. When filling of venous drainage was slow, simultaneous visualization prevented discrimination of normal venous return. Thus, because the information 3D dynamic MRA provides is not sufficient to determine treatment, it is not an alternative to conventional angiography, though it does play an important role in screening. The number of subjects included in this study was limited, and there was no evidence of statistically significant differences between some of the results. In addition, there were technical limitations of the definite imaging area and relatively low temporal resolution in exchange for spatial resolution.

Although twenty-three 3D dynamic MRA examinations were performed in 14 patients with DAVFs of the cavernous sinuses after embolization, its utility was not demonstrated until further confirmation by repeat angiography. However, the evaluation of the shunts was feasible, so it is anticipated that this imaging technique can be used to detect subclinical recurrence on posttreatment follow-up. We believe that the improvement in the spatial and temporal resolution on 3D dynamic MRA in the future will enable assessment of the entry points of DAVFs of the cavernous sinuses.

Conclusion

In this small series, 3D dynamic MRA enabled the direct demonstration of DAVFs of the cavernous sinuses and has improved diagnostic capability, compared with FSE T2WI and

TOF MRA. In addition, it may provide information about main venous drainage. Although bolus administration of contrast material is indispensable to 3D dynamic MRA, there is no need for a new program; and a brief required time period will facilitate using this technique for screening before conventional angiography.

Acknowledgments

We thank Takaharu Shonai, MD, PhD, Taishi Satoh, MD, and Yuriko Kawaai, MD, for assistance in preparation of the manuscript; and Ryuji Shirase, RT, and Kuniaki Harada, RT, for their technical ingenuity in the setting of parameters for the imaging protocol.

References

1. Barrow DL, Spector RH, Braun IF, et al. **Classification and treatment of spontaneous carotid-cavernous sinus fistulas.** *J Neurosurg* 1985;62:248–56
2. Halbach VV, Higashida RT, Hieshima GB, et al. **Dural fistulas involving the cavernous sinus: results of treatment in 30 patients.** *Radiology* 1987;163:437–42
3. Chen YW, Jeng JS, Liu HM, et al. **Carotid and transcranial color-coded duplex sonography in different types of carotid-cavernous fistula.** *Stroke* 2000;31:701–06
4. Kurata A, Takano M, Tokiwa K, et al. **Spontaneous carotid cavernous fistula presenting only with cranial nerve palsies.** *AJNR Am J Neuroradiol* 1993;14:1097–101
5. Stiebel-Kalish H, Setton A, Nimii Y, et al. **Cavernous sinus dural arteriovenous malformations: patterns of venous drainage are related to clinical signs and symptoms.** *Ophthalmology* 2002;109:1685–91
6. Wu HC, Ro LS, Chen CJ, et al. **Isolated ocular motor nerve palsy in dural carotid-cavernous sinus fistula.** *Eur J Neurol* 2006;13:1221–25
7. Hirabuki N, Miura T, Mitomo M, et al. **MR imaging of dural arteriovenous malformations with ocular signs.** *Neuroradiology* 1988;30:390–94
8. Chen JC, Tsuruda JS, Halbach VV. **Suspected dural arteriovenous fistula: results with screening MR angiography in seven patients.** *Radiology* 1992;183:265–71
9. Komiyama M, Fu Y, Yagura H, et al. **MR imaging of dural AV fistulas at the cavernous sinus.** *J Comput Assist Tomogr* 1990;14:397–401
10. Hirai T, Korogi Y, Hamatake S, et al. **Three-dimensional FISP imaging in the evaluation of carotid cavernous fistula: comparison with contrast-enhanced CT and spin-echo MR.** *AJNR Am J Neuroradiol* 1998;19:253–59
11. Ouanounou S, Tomsick TA, Heitsman C, et al. **Cavernous sinus and inferior petrosal sinus flow signal on three-dimensional time-of-flight MR angiography.** *AJNR Am J Neuroradiol* 1999;20:1476–81
12. Paksoy Y, Genc BO, Genc E. **Retrograde flow in the left inferior petrosal sinus and blood steal of the cavernous sinus associated with central vein stenosis: MR angiographic findings**. *AJNR Am J Neuroradiol* 2003;24:1364–68
13. Sakamoto M, Taoka T, Iwasaki S, et al. **Paradoxical parasellar high signals resembling shunt diseases on routine 3D time-of-flight MR angiography of the brain: mechanism for the signals and differential diagnosis from shunt diseases.** *Magn Reson Imaging* 2004;22:1289–93
14. Tsuchiya K, Katase S, Yoshino A, et al. **MR digital subtraction angiography of cerebral arteriovenous malformations.** *AJNR Am J Neuroradiol* 2000;21:707–11
15. Aoki S, Yoshikawa T, Hori M, et al. **MR digital subtraction angiography for the assessment of cranial arteriovenous malformations and fistulas.** *AJR Am J Roentgenol* 2000;175:451–53
16. Griffiths PD, Hoggard N, Warren DJ, et al. **Brain arteriovenous malformations: assessment with dynamic MR digital subtraction angiography.** *AJNR Am J Neuroradiol* 2000;21:1892–99
17. Coley SC, Romanowski CA, Hodgson TJ, et al. **Dural arteriovenous fistulae: noninvasive diagnosis with dynamic MR digital subtraction angiography.** *AJNR Am J Neuroradiol* 2002;23:404–07
18. Mori H, Aoki S, Okubo T, et al. **Two-dimensional thick-slice MR digital subtraction angiography in the assessment of small to medium-size intracranial arteriovenous malformations.** *Neuroradiology* 2003;45:27–33. Epub 2003 Jul 19
19. Farb RI, McGregor C, Kim JK, et al. **Intracranial arteriovenous malformations: real-time auto-triggered elliptic centric-ordered 3D gadolinium-enhanced MR angiography—initial assessment.** *Radiology* 2001;220:244–51
20. Gauvrit JY, Oppenheim C, Nataf F, et al. **Three-dimensional dynamic magnetic resonance angiography for the evaluation of radiosurgically treated cerebral arteriovenous malformations.** *Eur Radiol* 2006;16:583–91
21. Bonneville JF, Cattin F, Racle A, et al. **Dynamic CT of the laterosellar extradural venous spaces.** *AJNR Am J Neuroradiol* 1989;10:535–42
22. Milburn JM, Moran CJ, Cross DT 3rd, et al. **Effect of intraarterial papaverine on cerebral circulation time.** *AJNR Am J Neuroradiol* 1997;18:1081–85
23. Kim JK, Farb RI, Wright GA. **Test bolus examination in the carotid artery at dynamic gadolinium-enhanced MR angiography.** *Radiology* 1998;206:283–89
24. Borden JA, Wu JK, Shucart WA. **A proposed classification for spinal and cranial dural arteriovenous fistulous malformations and implications for treatment.** *J Neurosurg* 1995;82:166–79
25. Metz CE, Herman BA, Shen JH. **Maximum likelihood estimation of receiver operating characteristic (ROC) curves from continuously-distributed data.** *Stat Med* 1998;17:1033–53
26. Obuchowski NA. **Receiver operating characteristic curves and their use in radiology.** *Radiology* 2003;229:3–08
27. Kundel HL, Polansky M. **Measurement of observer agreement.** *Radiology* 2003;228:303–08
28. Takahashi S, Tomura N, Watarai J, et al. **Dural arteriovenous fistula of the cavernous sinus with venous congestion of the brain stem: report of two cases.** *AJNR Am J Neuroradiol* 1999;20:886–88